

# Fuel-Efficient Pulse Command Profiles for Flexible Spacecraft

William Singhose,\* Kristen Bohlke,† and Warren Seering‡  
*Massachusetts Institute of Technology, Cambridge, Massachusetts 02141*

A procedure for designing command profiles for flexible spacecraft is presented. The command profiles are designed to maneuver a spacecraft with very little residual vibration, even in the presence of modeling errors. To model the case where a spacecraft is equipped with on-off reaction jets, the command signals are restricted to positive or negative constant-amplitude pulses. The technique results in command profiles that are much more fuel efficient than the time-optimal commands, yet do not incur a significant time penalty. Robustness to modeling errors of both the time-optimal and the fuel-efficient commands are shown to be highly dependent on move distance; however, the fuel-efficient profiles are always as robust as the time-optimal profiles.

## I. Introduction

THE development of command profiles to maneuver flexible spacecraft is an area of active research. Recently, the technique of input shaping has been successfully applied to this problem. Input shaping allows the spacecraft to be maneuvered with little residual vibration, even in the presence of modeling errors.<sup>1–5</sup>

The process of input shaping can be summarized as follows. First, equations describing the dynamic response of the system to a sequence of impulses are formulated. Second, the dynamic equations are solved for an impulse sequence (an input shaper) that yields a small amount of residual vibration. Third, the input shaper is convolved with a desired input to form a shaped command. Finally, the shaped input is used to command the system. The shaped input has the same vibration reducing properties as the input shaper.<sup>6</sup>

Input shaping has been investigated and extended by many researchers since the original presentation by Singer and Seering.<sup>6</sup> Singhose et al.<sup>7,8</sup> proposed a technique for improving insensitivity to modeling errors. Hyde and Seering<sup>9</sup> demonstrated the input shaping process on multiple-mode systems. Jansen<sup>10</sup> and Magee and Book<sup>11</sup> used input shaping on long-reach manipulators.

Several researchers have presented methods for designing input shapers in the  $z$  plane.<sup>12–14</sup> Input shapers containing negative impulses were shown to improve rise time.<sup>15</sup> Input shaping was shown to be beneficial for trajectory following.<sup>16,17</sup>

In its most general form, the input shaping process leads to variable-amplitude command signals, which flexible spacecraft equipped with on-off jets cannot produce. Approximate methods for using shaping on constant-amplitude actuators have been developed.<sup>18,19</sup> Input shaping can be rigorously applied to the problem of controlling flexible spacecraft equipped with on-off reaction jets by requiring the impulses in the input shaper to have specific amplitudes.<sup>4</sup> The set of constraint equations governing the dynamic response and the impulse amplitudes can be solved with a standard optimization program. Input shaping for constant-amplitude actuators is equivalent to the time-optimal control for a certain class of flexible structures.<sup>20</sup>

This paper will present a novel procedure for designing command profiles that are considerably more fuel efficient than previously reported methods. The command profiles that are generated by the new technique are nearly time optimal. If the large fuel savings are considered, the new command profiles are very attractive alternatives to the time-optimal solutions.

This paper also demonstrates that the robustness of constant-amplitude input shaping shown previously in the literature is not

representative of the general problem. The method's robustness is highly dependent on the rest-to-rest slew displacement or the terminal velocity in a spin-up maneuver.

The simple model representing a flexible spacecraft that has been used previously in the literature<sup>2–5</sup> will be used again to evaluate the new profiles and to compare their performance with the techniques previously reported. The simplicity of the model should not reduce the usefulness of the proposed techniques for real hardware. Very accurate, nonlinear simulations of the Space Shuttle and hardware experiments have been conducted to verify that the input shaping techniques developed for the simple model can be easily extended to complex systems.<sup>4</sup>

## II. Fuel-Efficient Spin-Up Profiles

The new fuel-efficient command profiles will be generated for the system model shown in Fig. 1. This model represents a system with a single flexible mode and a rigid-body mode. A force input  $u(t)$  acts on mass  $m_1$  with an amplitude of  $u_{\max}$ , 0, or  $-u_{\max}$ . We have left out damping to simplify the development; however, the technique can be used with damped systems by simply adding damping terms in the constraint equations.<sup>3,6</sup> If the system under consideration has multiple modes, then dynamic constraint equations governing each mode are added to the problem formulation.<sup>4,5</sup>

The command profiles presented here are obtained by solving a set of constraint equations. The equations can be categorized as follows: 1) constraints on rigid body motion, 2) residual vibration constraints, 3) robustness constraints, 4) constraints on the impulse amplitudes, and 5) a time-optimality constraint.

To ensure that the desired rigid-body response is attained, the following equation must be satisfied:

$$v_d = \int \frac{u(t)}{(m_1 + m_2)} dt \quad (1)$$

where  $v_d$  is the desired spin-up velocity in units of (force)(time)/mass.

The desired rigid-body motion is set by Eq. (1); however, the main purpose of input shaping is to limit the amount of residual vibration that occurs when the system reaches its desired setpoint. The vibration equations can be nondimensionalized by using the ratio of vibration caused by the input shaper to the vibration caused by a single impulse.<sup>21</sup> This percentage residual vibration for a shaper containing  $n$  impulses is

$$V(\omega) = \sqrt{[\sum A_i \sin(\omega t_i)]^2 + [\sum A_i \cos(\omega t_i)]^2} \quad (2)$$

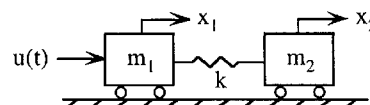


Fig. 1 Simple system model.

Received May 10, 1995; revision received Nov. 9, 1995; accepted for publication Jan. 30, 1996. Copyright © 1996 by the American Institute of Aeronautics and Astronautics, Inc. All rights reserved.

\*Research Assistant, Department of Mechanical Engineering. Member AIAA.

†Research Assistant, Department of Mechanical Engineering.

‡Professor, Department of Mechanical Engineering.

where  $i = 1, \dots, n$ ,  $A_i$  is the amplitude of the  $i$ th impulse,  $t_i$  is the time location of the  $i$ th impulse, and  $\omega$  is the natural frequency of the system. To include damping in the problem, simply use the damped version of Eq. (2) found in Refs. 3 and 6. By including Eq. (2) in our set of constraint equations, we can set the level of vibration to the quantity  $V$  when the system's frequency is exactly  $\omega$  (e.g., when  $V = 0.05$ , the shaped residual vibration amplitude is 5% of the baseline vibration amplitude). When  $V$  is set equal to zero and the constraint equations are solved for  $A_i$  and  $t_i$  while minimizing the shaper duration, the resulting input shaper is called a zero vibration (ZV) shaper. The shaper duration is minimized so that the shortest command that meets the performance criteria will be obtained.

If the system frequency varies from  $\omega$ , then there may exist a large amount of residual vibration. Equation (2) only guarantees a low level of vibration when the actual frequency equals the modeling frequency. One way to make an input shaper robust to modeling errors is to differentiate the vibration equation with respect to  $\omega$  and set the result equal to zero<sup>6</sup>:

$$\frac{d}{d\omega} \sqrt{[\sum A_i \sin(\omega t_i)]^2 + [\sum A_i \cos(\omega t_i)]^2} = 0 \quad (3)$$

When both Eqs. (2) and (3) are used with  $V = 0$ , the resulting shaper is called the zero vibration and derivative (ZVD) shaper.

Input shapers that are more robust than the ZVD shapers have been proposed.<sup>4,7,8</sup> Although the constraints associated with these shapers are generally better, they will not be presented in this paper, so that we may focus on fuel-efficiency issues.

To compare the performance of the ZV and ZVD input shapers in the presence of modeling errors, we examine the shapers' sensitivity curves, which are plots of the vibration amplitude as a function of normalized system frequency ( $\omega_{\text{actual}}/\omega_{\text{model}}$ ). Typical sensitivity curves for ZV and ZVD shapers are shown in Fig. 2. Clearly, the ZVD shaper keeps the vibration amplitude at a low level over a wider range of frequencies than the ZV shaper. The robustness of the two shapers can be compared quantitatively by defining the insensitivity of a shaper as the width of its sensitivity curve at a low level of vibration. For example, the 5% insensitivity (the width at 0.05) of the ZV shaper is 0.053, whereas the 5% insensitivity of ZVD shaper is 0.252.

Equations (1–3) control the rigid and flexible dynamics; however, the actuator limitations have not been addressed. Our model requires a constant magnitude command, i.e.,  $u(t)$  is restricted to have a value of  $+u_{\text{max}}$ , 0, or  $-u_{\text{max}}$ . Commands consisting of constant-amplitude pulses can be generated with input shaping if constraints are placed on the amplitudes of the impulses in the input shaper. For maneuvers that spin up to a constant velocity, the time-optimal command consists of a series of alternating positive and negative pulses of variable length, with one more positive pulse than negative pulse.<sup>3,4</sup> Therefore, to generate the time-optimal command for spin-up maneuvers, an input shaper must have the form

$$\begin{bmatrix} A_i \\ t_i \end{bmatrix} = \begin{bmatrix} 1 & -2 & 2 & -2 & \dots & 2 & -1 \\ 0 & t_2 & t_3 & t_4 & \dots & t_{n-1} & t_n \end{bmatrix} \quad (4)$$

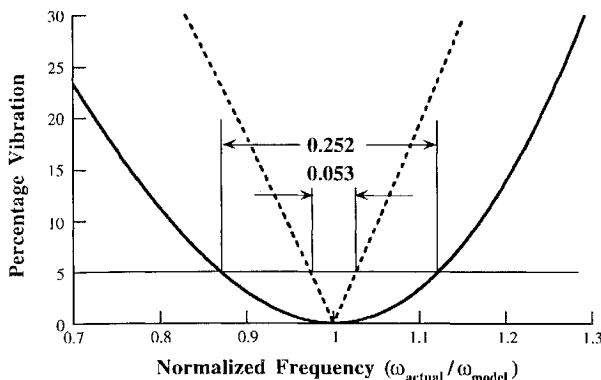


Fig. 2 Sensitivity curves for ZV and ZVD input shapers: - - -, ZV and —, ZVD.

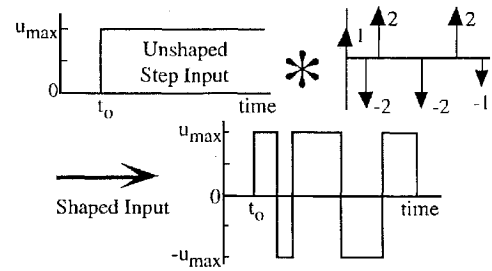


Fig. 3 Using input shaping to generate a time-optimal spin-up profile.

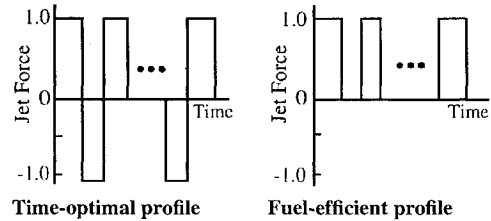


Fig. 4 Spin-up command profiles.

where  $n$  is even. Furthermore, the shaper given by Eq. (4) must be convolved with a step input of magnitude  $u_{\text{max}}$ . This procedure is demonstrated in Fig. 3. The value of  $n$  in the given shaper depends on the type of dynamic constraints that are used in the shaper design and the desired spin-up velocity. For the ZV constraints and small terminal velocities, the value of  $n$  is four. That is, the time-optimal ZV shaper for low-velocity spin-up profiles is

$$\begin{bmatrix} A_i \\ t_i \end{bmatrix} = \begin{bmatrix} 1 & -2 & 2 & -1 \\ 0 & t_2 & t_3 & t_4 \end{bmatrix} \quad (5)$$

where the values of  $t_2$  through  $t_4$  are determined by solving Eqs. (1) and (2). Note that Eq. (2) is actually two constraint equations when  $V = 0$  because both the sine and cosine sums must equal zero independently. The time-optimal ZVD shaper will have a different number of impulses because of the additional constraints associated with Eq. (3).

The new shapers to be developed in this paper are motivated by the fact that the time-optimal command profiles use fuel throughout their duration. We postulate that command profiles that contain only positive pulses and allow periods of coasting can robustly reduce residual vibration while being only slightly longer than the time-optimal commands. We propose the following fuel-efficient shaper:

$$\begin{bmatrix} A_i \\ t_i \end{bmatrix} = \begin{bmatrix} 1 & -1 & \dots & 1 & -1 \\ 0 & t_2 & \dots & t_{n-1} & t_n \end{bmatrix} \quad (6)$$

The command profile generated by Eq. (6) is compared to the time-optimal profile in Fig. 4. Unlike the fuel-efficient profile, the time-optimal profile generates forces in the direction opposite to the desired velocity. Although negative pulses are required to slow down a system in rest-to-rest slews, they are not required for spin-up maneuvers. The presence of the negative pulses in spin-up commands leads to large fuel expenditures.

Note that a command profile that contains only positive pulses is not only more fuel-efficient than the time-optimal command, it is the fuel-optimal solution. The final velocity is simply the time integral of the command profile divided by the system mass; see Eq. (1). Therefore, for a given spin-up velocity, fuel usage is minimized when the command contains only positive pulses.

Because of the transcendental nature of Eqs. (2) and (3), there are an infinite number of solutions to the given constraints. To obtain the time-optimal solution, the duration of the shaper must be as short as possible. This leads to the final constraint that must be optimized,

$$\min(t_n) \quad (7)$$

Shaped profiles were designed for the system of Fig. 1 with parameter values  $m_1 = m_2 = k = u_{\text{max}} = 1$ . The shapers were determined by solving the appropriate constraint equations with the nonlinear

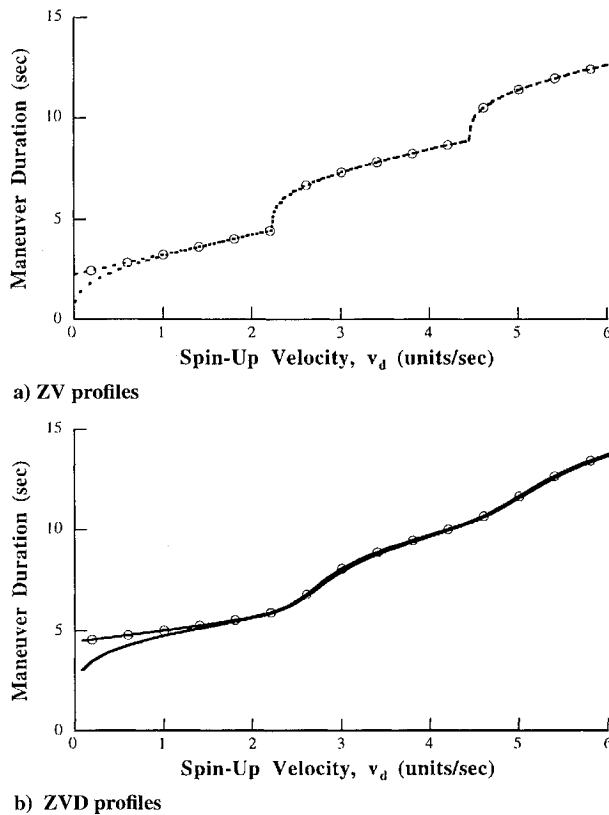


Fig. 5 Maneuver times of the time-optimal and fuel-efficient spin-up profiles: ---, time-optimal ZV; -○-, fuel-efficient ZV; —, time-optimal ZVD; and —○—, fuel-efficient ZVD.

optimization program GAMS.<sup>22</sup> The time-optimal ZV profile is obtained by using Eqs. (1), (2), (4), and (7), whereas the time-optimal ZVD is obtained by adding Eq. (3). The fuel-efficient profiles are obtained by replacing Eq. (4) with Eq. (6).

Because nonlinear optimization is susceptible to local minima, the solutions obtained from the optimization may not be time optimal. Fortunately, a method for verifying the time optimality of a candidate solution is available.<sup>20</sup> The verification method is based on sufficient and necessary conditions obtained from Pontryagin's maximum principle. Using the method described in the reference, we have verified the accuracy of the time-optimal solutions presented here. Unfortunately, no such verification method is available for the fuel-efficient profiles. We will see, however, that the fuel-efficient profiles are so very close to time optimal that it is improbable that a shorter fuel-efficient solution exists. In fact, for certain parameter values, the fuel-efficient profile is exactly equal to the time-optimal profile.

Given that we are suggesting that time optimality be sacrificed for fuel efficiency, we will first examine the cost of the new shapers in terms of the maneuver time. Figure 5 compares the command durations for the time-optimal and fuel-efficient ZV and ZVD profiles for the range of  $0.1 \leq v_d \leq 6$ . Figure 5a reveals that the fuel-efficient ZV profiles are essentially time optimal for all spin-up velocities greater than about 1 unit/s. For velocities greater than 1.2, the length of the fuel-efficient profile is at most 1.2% longer than the time-optimal profile. Furthermore, the average duration is only 0.24% longer than the time optimal over the range  $1.2 \leq v_d \leq 6$ .

Figure 5b shows that the fuel-efficient ZVD profiles are nearly time optimal for all spin-up velocities greater than about 1.5 units/s. After  $v_d = 1.7$ , the length of the fuel-efficient profile is at most 1.8% longer than the time-optimal profile, whereas the average duration is only 1.0% longer than the time optimal over the range  $1.7 \leq v_d \leq 6$ . (Whenever possible, dashed lines will be used to represent ZV profiles and solid lines will be used for ZVD profiles. Additionally, open circles will be added to curves representing fuel-efficient profiles.)

The fuel usage of the time-optimal and the fuel-efficient shapers are compared in Fig. 6. Fuel usage is measured as the cumulative

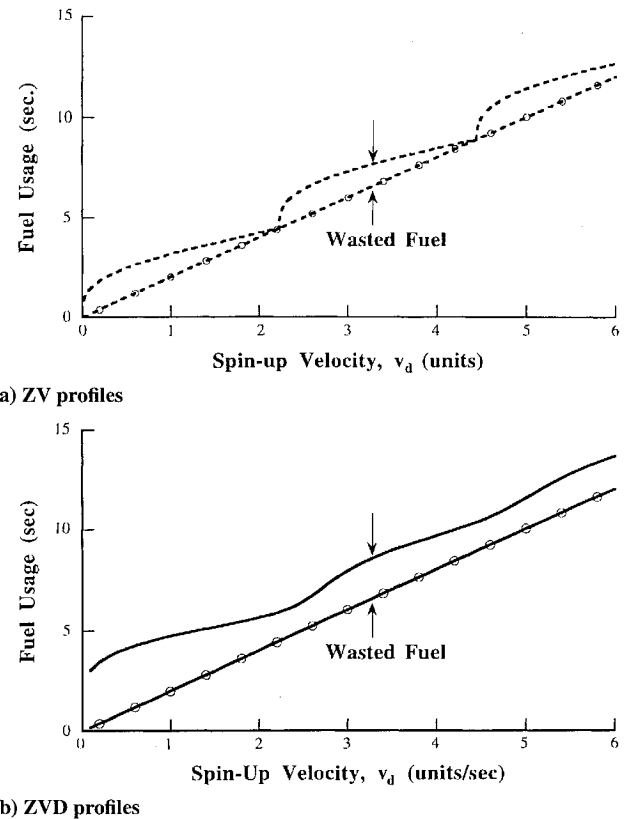


Fig. 6 Fuel usage of the time-optimal and fuel-efficient spin-up profiles: ---, time-optimal ZV; -○-, fuel-efficient ZV; —, time-optimal ZVD; and —○—, fuel-efficient ZVD.

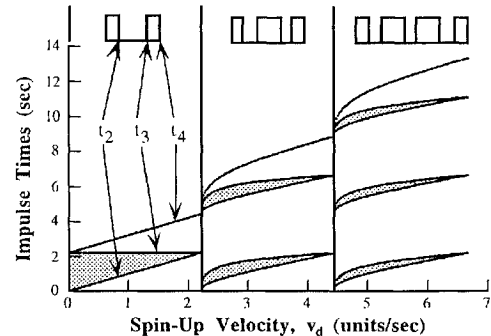


Fig. 7 Impulse times for the fuel-efficient ZV spin-up profiles; shaded areas indicate periods of coasting.

time that the actuator is turned on. The proposed fuel-efficient profiles use less fuel than their time-optimal counterparts at all velocities. At low spin-up velocities, the fuel usage is reduced by an order of magnitude. At higher velocities the percentage savings decreases, but it is still substantial. Because the fuel-efficient profiles are essentially time optimal for most velocities, the difference in fuel usage can be regarded as wasted fuel.

Given the significant fuel savings associated with the fuel-efficient profiles, it is surprising that they are so close to time optimal. By examining the structure of the shapers we can develop a better understanding of this unexpected result. Figure 7 shows the impulse times for the fuel-efficient ZV shaper as a function of spin-up velocity. As the velocity is increased, the number of pulses in the profile increases. This transition is shown along the top of the figure. The shaded areas indicated periods of coasting.

Figure 8 compares the impulse times of the fuel-efficient and time-optimal ZV shapers. The impulses of both shapers evolve in a similar fashion. After the first region, the fuel-efficient profiles are very nearly the time-optimal profiles with the negative pulses removed. Put simply, the fuel-efficient profiles tend to coast, whereas the time-optimal profiles decelerate. The same final velocity is obtained

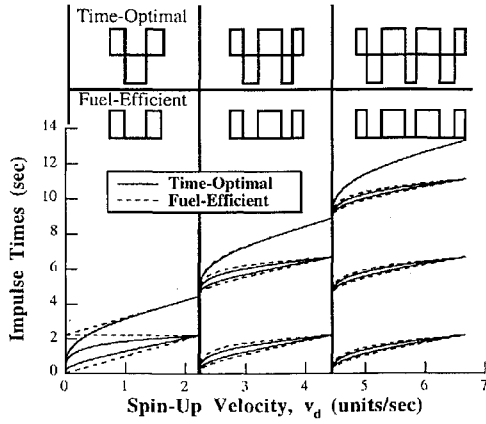


Fig. 8 Comparison of fuel-efficient and time-optimal ZV impulse times.

because the deceleration pulses are offset by longer acceleration periods in the time-optimal profiles. If the duration of the negative pulses is subtracted from the positive pulses, then the resulting time period will equal the duration of the fuel-efficient pulses.

### III. Fuel-Efficient Rest-to-Rest Profiles

If the desired spacecraft maneuver is a rest-to-rest slew rather than a velocity spin up, the input shapers used to construct the command must have a different form than the spin-up shapers. The command profiles must contain negative pulses. The difference arises out of the constraint equations that govern the two problems. In addition to the constraints used for the spin up [Eqs. (1–3)], the rigid-body displacement at the end of the command must also be controlled. The rigid-body displacement is described by

$$x_d = \int \int \frac{u(t)}{(m_1 + m_2)} dt dt \quad (8)$$

where  $x_d$  is the desired move distance in units of (force)(time<sup>2</sup>)/mass. In addition to setting  $x_d$ , rest-to-rest slews require  $v_d = 0$  in Eq. (1), i.e., the final velocity must be zero.

The time-optimal rest-to-rest command is a series of alternating positive and negative pulses.<sup>2–4,23–25</sup> Therefore, the time-optimal ZV and ZVD shapers for rest-to-rest slews must have the form

$$\begin{bmatrix} A_i \\ t_i \end{bmatrix} = \begin{bmatrix} 1 & -2 & 2 & \cdots & -2 & 1 \\ 0 & t_2 & t_3 & \cdots & t_{n-1} & t_n \end{bmatrix} \quad (9)$$

where  $n$  is odd.

Once again, we postulate that command profiles, which allow periods of coasting, can robustly reduce residual vibration, while being only slightly longer than the time-optimal commands. The fuel-efficient shapers we propose for rest-to-rest maneuvers that meet the ZV and ZVD constraints have the form

$$\begin{bmatrix} A_i \\ t_i \end{bmatrix} = \begin{bmatrix} 1 & -1 & 1 & \cdots & -1 & -1 & \cdots & -1 & 1 \\ 0 & t_2 & t_3 & \cdots & t_{n/2} & t_{(n/2)+1} & \cdots & t_{n-1} & t_n \end{bmatrix} \quad (10)$$

Figure 9 compares the proposed fuel-efficient rest-to-rest shapers to their time-optimal counterparts. The inherent fuel efficiency of the new shapers is readily apparent. The pulses that cause acceleration in the desired direction all occur before the deceleration pulses.

Note that, unlike the fuel-efficient spin-up profiles, the fuel-efficient rest-to-rest profiles are not the fuel-optimal solution. In fact, the fuel-optimal solution for rest-to-rest moves is undefined. As the fuel usage is decreased, the pulses get narrower and the coast periods get longer. In the limit, the pulse widths go to zero and the coast periods go to infinity.

The time-optimal and fuel-efficient rest-to-rest shapers were determined for the system of Fig. 1 with parameters  $m_1 = m_2 = k = u_{\max} = 1$ . Figure 10 compares the command durations for the time-optimal and fuel-efficient ZV and ZVD rest-to-rest profiles for the range of  $0.1 \leq x_d \leq 40$ . The time penalties associated

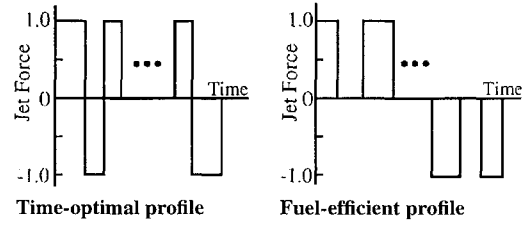
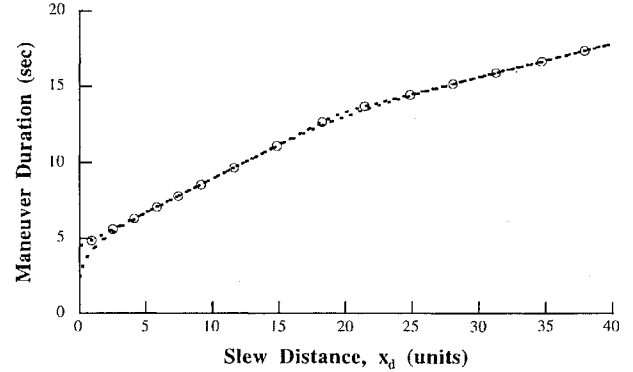
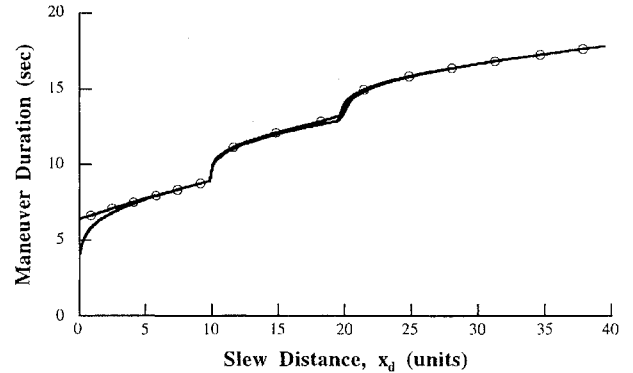


Fig. 9 Rest-to-rest command profiles.



a) ZV profiles



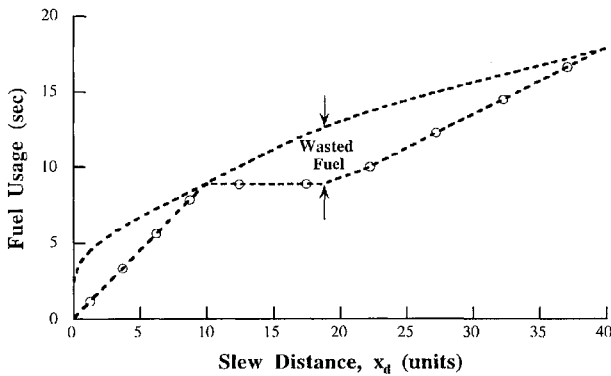
b) ZVD profiles

Fig. 10 Maneuver times of the rest-to-rest profiles: ---, time-optimal ZV; -◇-, fuel-efficient ZV; —, time-optimal ZVD; and —○—, fuel-efficient ZVD.

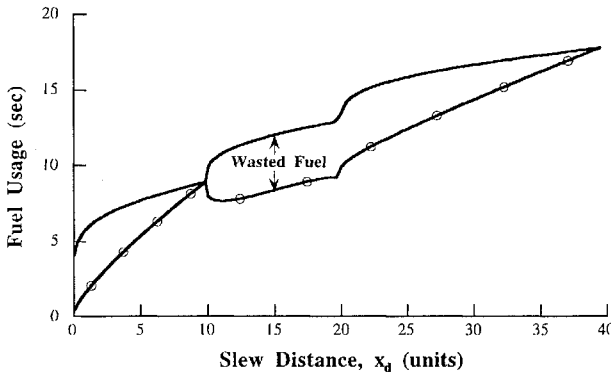
with the fuel-efficient rest-to-rest shapers are almost negligible. For  $x_d \geq 3.0$ , the fuel-efficient ZV profile is at most 2.3% longer than time optimal, and the fuel-efficient ZVD is at most 4.2% longer. Over the range  $3 \leq x_d \leq 40$ , the fuel-efficient ZV profile averages 0.5% longer than the time optimal, whereas the fuel-efficient ZVD profile averages 0.6% longer.

The fuel saved by the new rest-to-rest shapers depends on desired slew distance just as the fuel savings of the spin-up shapers depended on spin-up velocity. The fuel usage of the time-optimal and the fuel-efficient ZV and ZVD rest-to-rest shapers are compared in Fig. 11. For all values of slew distance the fuel-efficient profiles use less fuel than their time-optimal counterparts. At small distances, the fuel usage is reduced by an order of magnitude. Over most of the move distances, the fuel savings averages about 3 s.

To gain a better appreciation for the fuel-efficient solution, we can plot the time locations of the shaper's impulses as a function of slew distance. Figure 12 shows these times for the fuel-efficient ZVD profiles. The structure of the command profile has been plotted along the top of the figure. For small slew distances, the command profile is composed of two positive pulses followed immediately by two negative pulses. For the intermediate slew distances, there is a period of coasting between positive and negative pulses. Finally, for long slews the profile is three positive pulses followed immediately by three negative pulses. The curves representing the impulse times in Fig. 12 evolve in a repetitive fashion. As slew distance is increased, impulse times converge and then give rise to additional impulses,



a) ZV profiles



b) ZVD profiles

Fig. 11 Fuel usage of the time-optimal and fuel-efficient rest-to-rest profiles: ----, time-optimal ZV; -○-, fuel-efficient ZV; —, time-optimal ZVD, and —○—, fuel-efficient ZVD.

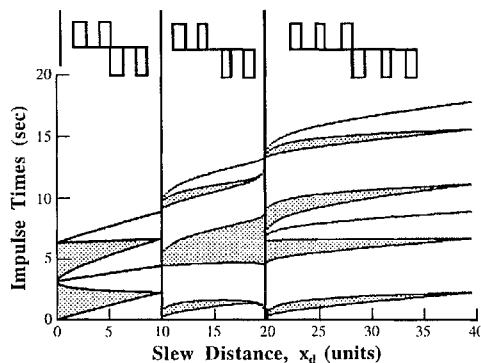


Fig. 12 Impulse times for the fuel-efficient ZVD rest-to-rest profiles; shaded areas indicate periods of coasting.

which represent additional coast periods or additional pulses. The shaded regions of the figure indicate periods of coasting between pulses.

#### IV. Variation of Insensitivity

In most previous work using input shaping to generate command profiles for flexible spacecraft it was assumed that using ZVD constraints would guarantee good robustness to modeling errors. This is not the case, because the insensitivity of input shapers varies with spin-up velocity and slew distance. For certain move distances, the ZVD shaper will have relatively poor robustness to modeling errors. In this section we will explore the variation of insensitivity. Two important comparisons will be made, the comparison between the insensitivity of ZV and ZVD shapers and the comparison between fuel-efficient and time-optimal shapers.

##### Spin-Up Profiles

Figure 13 shows the 5% insensitivity of the fuel-efficient and time-optimal spin-up profiles. The 5% insensitivity was calculated by

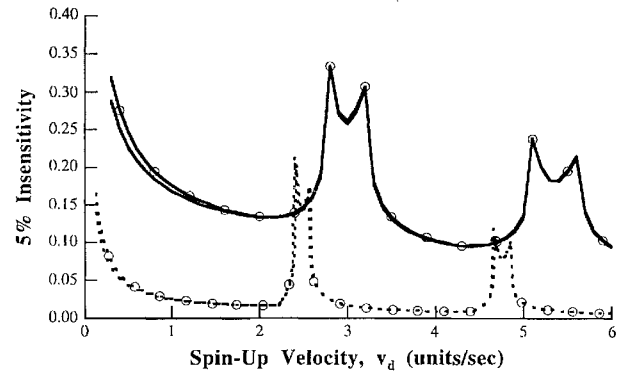


Fig. 13 Insensitivity of spin-up profiles as a function of spin-up velocity: ----, time-optimal ZV; -○-, fuel-efficient ZV; —, time-optimal ZVD; and —○—, fuel-efficient ZVD.

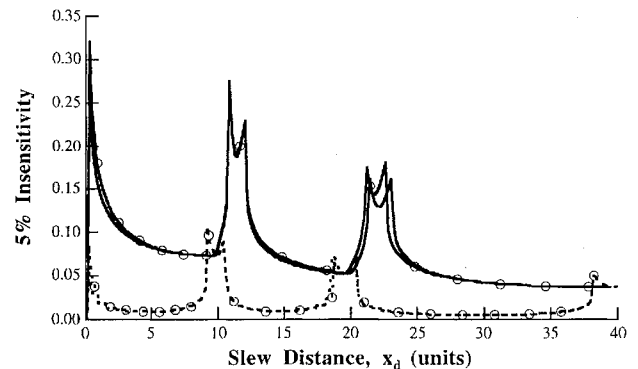


Fig. 14 Insensitivity of rest-to-rest profiles as a function of slew distance: ----, time-optimal ZV; -○-, fuel-efficient ZV; —, time-optimal ZVD; and —○—, fuel-efficient ZVD.

computing the sensitivity curve for each shaper and spin-up velocity, and then measuring the width of the curve at 0.05. This measurement tells us over what frequency range the residual vibration will be below 0.05. The larger the value of insensitivity, the more robust the shaper will be to modeling errors.

Figure 13 demonstrates that insensitivity varies considerably with spin-up velocity. For example, the ZVD shaper is three times more robust for velocities near 3 units/s than for velocities close to 4 units/s. Even though the insensitivity of the ZVD shaper varies with spin-up velocity, it is almost always significantly larger than for the ZV shaper. Figure 13 also demonstrates that the fuel-efficient shapers have essentially the same robustness as the time-optimal shapers.

##### Rest-to-Rest Profiles

Figure 14 shows the 5% insensitivity of the fuel-efficient and time-optimal rest-to-rest profiles. As expected, the ZVD shapers are significantly more robust than the ZV shapers. Once again, the fuel-efficient shapers have essentially the same insensitivity as the time-optimal shapers.

Given that insensitivity can be relatively small for certain spin-up velocities and slew distances, there is justification for shapers that are even more robust than the ZVD shaper. In fact, a procedure for developing extra-insensitive shapers has been reported.<sup>4,7,8</sup>

#### V. Simulation Evaluations

Experiments using Draper Laboratory's simulation of the Space Shuttle's remote manipulator and a flexible hardware testbed have verified the benefits of using input shaping with constant-amplitude actuators.<sup>4</sup> The simulations used to test the theoretical results of this paper will be restricted to simulations of the system shown in Fig. 1. If the trends in fuel savings and insensitivity are supported by these simulations, then given the previously reported experimental results, there is good reason to believe that the trends will also occur in more complicated hardware.

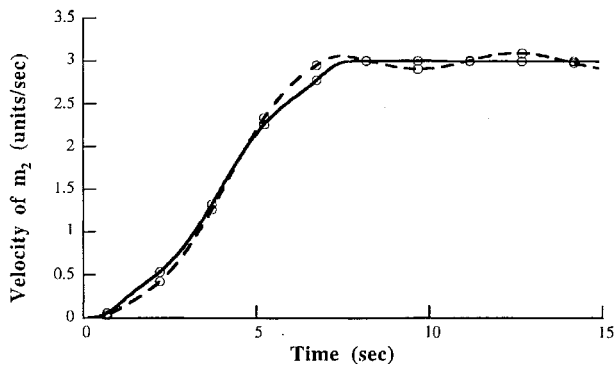


Fig. 15 Comparison of fuel-efficient and time-optimal ZVD responses with and without a modeling error: —, time optimal,  $k = 1.0$ ; —○—, fuel efficient,  $k = 1.0$ ; ---, time optimal,  $k = 0.6$ ; and -○-, fuel efficient,  $k = 0.6$ .

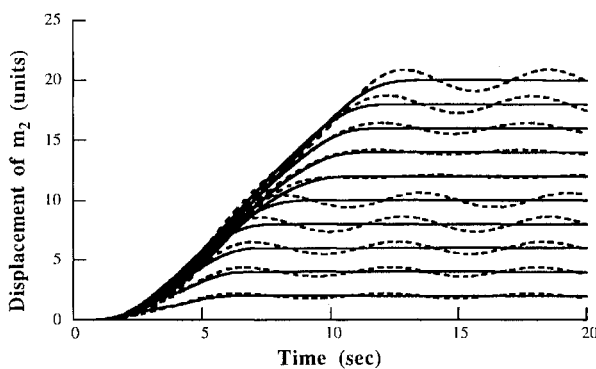


Fig. 16 Residual vibration as a function of slew distance (constant modeling error): —, fuel-efficient ZVD,  $k = 1.0$  and ---, fuel-efficient ZVD,  $k = 0.6$ .

Two important results of the theoretical development will be tested. First, we will verify that the fuel-efficient shaper yields the same rise time and insensitivity as the time-optimal shaper, even though it uses considerably less fuel. Second, the variation of insensitivity with maneuver distance will be investigated.

Simulations of the system shown in Fig. 1 were performed using the command profiles generated with the spin-up fuel-efficient and time-optimal ZVD shapers. Figure 15 compares the system response to the command profiles when the spin-up velocity is 3 units/s and the spring constant  $k$  is set equal to the values of 1.0 and 0.6. The responses with  $k = 1.0$  represent the case when the system model is exact. The data for  $k = 0.6$  represent the responses to a modeling error of 30%; the frequency shifts from 0.225 to 0.174 Hz. Figure 15 shows that the fuel-efficient shaper yields essentially the same response as the time-optimal shaper (the responses are indistinguishable on the graphs), even though it requires 1.9 fewer seconds of fuel. These results illustrate the information shown in Figs. 5 and 13.

Figure 16 shows the fuel-efficient ZVD responses for slew distances ranging from 2 to 20 units. The solid curves represent responses when the model is exact ( $k = 1.0$ ). The responses achieve the desired setpoint with zero residual vibration. The dashed lines correspond to responses when a modeling error is introduced by changing the spring constant to 0.6. Notice that for the same modeling error, the residual vibration varies significantly with slew distance, reaching a minimum at about 12 units. This result demonstrates that insensitivity to modeling errors is strongly dependent on slew distance, as was predicted by Fig. 14. The low level of vibration near 12 units was predicted by the large value of insensitivity shown at that value.

## VI. Conclusions

A new technique for designing command profiles for flexible spacecraft equipped with on-off reaction jets has been presented.

The technique can design command profiles for rest-to-rest slews or accelerations to constant velocity. The new profiles are significantly more fuel efficient than the time-optimal profiles, even though the commands are effectively the same length as the time-optimal commands. Additionally, the new profiles have essentially the same insensitivity to modeling errors as the time-optimal profiles. Other results demonstrate that insensitivity to modeling errors is highly dependent on slew distance and spin-up velocity. Computer simulations verified the effectiveness of the proposed command profiles.

## Acknowledgments

Support for this work was provided by the U.S. Office of Naval Research Fellowship Program and the Massachusetts Institute of Technology Space Engineering Research Center through NASA Grant NAGW-1335. The methods described in this paper are covered under issued and pending U.S. patents, including #4,916,635, April 10, 1990. Commercial use of these methods requires written permission from the Massachusetts Institute of Technology.

## References

- <sup>1</sup>Banerjee, A. K., "Dynamics and Control of the WISP Shuttle-Antennae System," *Journal of the Astronautical Sciences*, Vol. 41, No. 1, 1993, pp. 73-90.
- <sup>2</sup>Liu, Q., and Wie, B., "Robust Time-Optimal Control of Uncertain Flexible Spacecraft," *Journal of Guidance, Control, and Dynamics*, Vol. 15, No. 3, 1992, pp. 597-604.
- <sup>3</sup>Singh, T., and Vadali, S. R., "Robust Time-Optimal Control: A Frequency Domain Approach," *Journal of Guidance, Control, and Dynamics*, Vol. 17, No. 2, 1994, pp. 346-353.
- <sup>4</sup>Singhose, W., Derezinski, S., and Singer, N., "Extra-Insensitive Input Shapers for Controlling Flexible Spacecraft," *Journal of Guidance, Control, and Dynamics*, Vol. 19, No. 2, 1996, pp. 385-391.
- <sup>5</sup>Wie, B., Sinha, R., and Liu, Q., "Robust Time-Optimal Control of Uncertain Structural Dynamic Systems," *Journal of Guidance, Control, and Dynamics*, Vol. 15, No. 5, 1993, pp. 980-983.
- <sup>6</sup>Singer, N. C., and Seering, W. P., "Preshaaping Command Inputs to Reduce System Vibration," *Journal of Dynamic Systems, Measurement and Control*, Vol. 112, March 1990, pp. 76-82.
- <sup>7</sup>Singhose, W., Seering, W., and Singer, N., "Residual Vibration Reduction Using Vector Diagrams to Generate Shaped Inputs," *Journal of Mechanical Design*, Vol. 116, June 1994, pp. 654-659.
- <sup>8</sup>Singhose, W., Porter, L., and Singer, N., "Vibration Reduction Using Multi-Hump Extra-Insensitive Input Shapers," *Proceedings of the American Control Conference* (Seattle, WA), Inst. of Electrical and Electronics Engineers, Piscataway, NJ, 1995, pp. 3830-3834.
- <sup>9</sup>Hyde, J. M., and Seering, W. P., "Using Input Command Pre-Shaping to Suppress Multiple Mode Vibration," *Proceedings of the IEEE International Conference on Robotics and Automation* (Sacramento, CA), Inst. of Electrical and Electronics Engineers, New York, 1991, pp. 2604-2609.
- <sup>10</sup>Jansen, J. F., "Control and Analysis of a Single-Link Flexible Beam with Experimental Verification," Oak Ridge National Lab., ORNL/TM-12198, Oak Ridge, TN, 1992.
- <sup>11</sup>Magee, D. P., and Book, W. J., "Filtering Schilling Manipulator Commands to Prevent Flexible Structure Vibration," *Proceedings of the American Control Conference* (Baltimore, MD), Inst. of Electrical and Electronics Engineers, Piscataway, NJ, 1994, pp. 2538-2542.
- <sup>12</sup>Jones, S. D., and Ulsoy, A. G., "Control Input Shaping for Coordinate Measuring Machines," *Proceedings of the American Control Conference* (Baltimore, MD), Inst. of Electrical and Electronics Engineers, Piscataway, NJ, 1994, pp. 2899-2903.
- <sup>13</sup>Seth, N., Rattan, K. S., and Brandstetter, R. W., "Vibration Control of a Coordinate Measuring Machine," *IEEE Conference on Control Applications* (Dayton, OH), Inst. of Electrical and Electronics Engineers, New York, 1993, pp. 368-373.
- <sup>14</sup>Tuttle, T. D., and Seering, W. P., "A Zero-Placement Technique for Designing Shaped Inputs to Suppress Multiple-Mode Vibration," *Proceedings of the American Control Conference* (Baltimore, MD), Inst. of Electrical and Electronics Engineers, Piscataway, NJ, 1994, pp. 2533-2537.
- <sup>15</sup>Singhose, W., Singer, N., and Seering, W., "Design and Implementation of Time-Optimal Negative Input Shapers," *International Mechanical Engineering Congress and Exposition* (Chicago, IL), American Society of Mechanical Engineers, Fairfield, NJ, 1994, pp. 151-157 (DSC 55-1).
- <sup>16</sup>Drapeau, V., and Wang, D., "Verification of a Closed-Loop Shaped-Input Controller for a Five-Bar-Linkage Manipulator," *Proceedings of the IEEE International Conference on Robotics and Automation* (Atlanta, GA), Inst. of Electrical and Electronics Engineers, New York, 1993, pp. 216-221.

<sup>17</sup>Singhose, W., and Singer, N., "Initial Investigations into the Effects of Input Shaping on Trajectory Following," *Proceedings of the American Controls Conference* (Baltimore, MD), Inst. of Electrical and Electronics Engineers, Piscataway, NJ, 1994, pp. 2526-2532.

<sup>18</sup>Rogers, K., "Limiting Vibrations in Systems with Constant Amplitude Actuators Through Command Shaping," M.S. Thesis, Dept. of Mechanical Engineering, Massachusetts Inst. of Technology, Cambridge, MA, May 1994.

<sup>19</sup>Singhose, W., "A Vector Diagram Approach to Shaping Inputs for Vibration Reduction," MIT Artificial Intelligence Lab. Memo 1223, Massachusetts Inst. of Technology, Cambridge, MA, March 1994.

<sup>20</sup>Pao, L. Y., and Singhose, W. E., "On the Equivalence of Minimum Time Input Shaping with Traditional Time-Optimal Control," *IEEE Conference on Control Applications* (Albany, NY), Inst. of Electrical and Electronics

Engineers, New York, 1995, pp. 1120-1125.

<sup>21</sup>Bolz, R. E., and Tuve, G. L., *CRC Handbook of Tables for Applied Engineering Science*, CRC Press, Boca Raton, FL, 1973.

<sup>22</sup>Brooke, A., Kendrick, D., and Meeraus, A., *GAMS: A User's Guide*, Scientific, Redwood City, CA, 1988.

<sup>23</sup>Ben-Asher, J., Burns, J. A., and Cliff, E. M., "Time-Optimal Slewing of Flexible Spacecraft," *Journal of Guidance, Control, and Dynamics*, Vol. 15, No. 2, 1992, pp. 360-367.

<sup>24</sup>Pao, L. Y., "Characteristics of the Time-Optimal Control of Flexible Structures with Damping," *IEEE Conference on Control Applications* (Glasgow, Scotland, UK), Inst. of Electrical and Electronics Engineers, New York, 1994, pp. 1299-1304.

<sup>25</sup>Thompson, R. C., Junkins, J. L., and Vadali, S. R., "Near-Minimum Time Open-Loop Slewing of Flexible Vehicles," *Journal of Guidance, Control, and Dynamics*, Vol. 12, No. 1, 1989, pp. 82-88.

# Journey to the Moon

A History of the Apollo Spacecraft's Guidance Computer  
Eldon C. Hall

The first of its kind, *Journey to the Moon* details the history and design of the computer that enabled United States' astronauts to land on the moon. In describing the evolution of the Apollo Guidance Computer, Mr. Hall contends that the development of the Apollo computer supported and motivated the semiconductor industry during a period of time when integrated circuits were just emerging. This was the period just prior to the electronics revolution that gave birth to modern computers.



American Institute of Aeronautics and Astronautics  
Publications Customer Service, 9 Jay Gould Ct., P.O. Box 753, Waldorf, MD 20604  
Fax 301/843-0159 Phone 1-800/682-2422 8 a.m. - 5 p.m. Eastern

## MAJOR UNITS OF THE AGC GUIDANCE, NAVIGATION AND CONTROL SYSTEM

In addition, the book recalls the history of computer technology, both hardware and software, and the applications of digital computing to missile guidance systems and manned spacecraft. The book also offers graphics and photos drawn from the NASA archives which illustrate the technology and related events during the Apollo project.

Written for experts as well as lay persons, *Journey to the Moon* is the first book of its kind and a must for anyone interested in the history of science and the relevance of computer technology to space exploration.

1995

ISBN 1-56347-185-X

Order #: 85-X

Sales Tax: CA residents, 8.25%; DC, 6%. For shipping and handling add \$4.75 for 1-4 books (call for rates for higher quantities). Orders under \$100.00 must be prepaid. Foreign orders must be prepaid and include a \$20.00 postal surcharge. Please allow 4 weeks for delivery. Prices are subject to change without notice. Returns will be accepted within 30 days. Non-U.S. residents are responsible for payment of any taxes required by their government.